X-Band photonic microwaves with phase noise below −180 dBc/Hz using a free-running monolithic comb

MANOJ KALUBOVILAGE,[1,*] **MAMORU ENDO,**[2] **AND THOMAS R. SCHIBLI**[1,3]

[1] *Department of Physics, University of Colorado Boulder, Boulder, CO 80309, USA*
[2] *Department of Applied Physics, School of Engineering, The University of Tokyo, 7-3-1, Hongo, Bunkyo, Tokyo 113-8656, Japan*
[3] *JILA, University of Colorado, Boulder, CO 80309, USA*
*manoj.kalubovilage@colorado.edu

Abstract: Free-running mode-locked monolithic optical frequency combs offer a compact and simple alternative to complicated optical frequency division schemes. Ultra-low free-running noise performance of these oscillators removes the necessity of external phase stabilization, making the microwave systems uncomplicated and compact with lower power consumption while liberating the sidebands of the carrier from servo bumps typically present around hundreds of kilohertz offsets. Here we present a free-running monolithic laser-based 8 GHz photonic microwaves generation and characterization with a cryogenically cooled power splitter to demonstrate a state-of-the-art phase noise floor of less than −180 dBc/Hz below 1 MHz offset from the carrier.

1. Introduction

Photonics-based microwave generation brings the stability of photonic oscillators to the microwave domain. The stability and phase noise of the photonic systems outperform their traditional counterparts, such as room temperature sapphire whispering gallery mode oscillators, by several orders of magnitude [1–4]. This unequal performance of photonic microwaves will likely advance many fields such as communication [5], navigation [6], radar systems [7], time-frequency metrology [8–10]. In particular, frequency comb-based optical frequency division (OFD) schemes have demonstrated unprecedented stability and spectral purity in the microwave domain [1]. OFD systems rely on the high-quality factor of ultra-stable optical cavities. Optical frequency combs (OFCs) phase-locked to the optical cavity act as a phase-coherent link between optical and microwave regimes, transferring the stability of the optical cavity to the periodicity of the pulse train of the OFC. Photodetection of the pulse train produces the electrical spectrum consisting of the harmonics of the repetition rate of the optical pulses.

Despite the outstanding performance of full OFD systems, they are often complicated laboratory setups due to the requirements of high finesse cavities and active phase stabilization [1,2]. Easy to operate, fiber-based OFCs are attractive towards fieldable photonic microwave sources due to their compactness and robustness [11]. Er-fiber-based OFCs also have the advantage of 1550 nm center wavelengths for large-scale and low-cost pulse distribution. However, the relatively high intrinsic noise of fiber lasers requires tight external phase stabilization to optical cavities to achieve the desired ultra-low phase noise performance.

On the other hand, mode-locked monolithic lasers (MMLL) offer ultra-low noise performance without any phase noise stabilization [12,13]. The MMLL is built with a CaF_2 spacer as the laser cavity. CaF_2 offers excellent transparency and near-zero second-order dispersion at the wavelength of 1550 nm. The third-order dispersion is compensated through a Gires–Tournois

interferometer (GTI) coating deposited onto the CaF$_2$ spacer. The gain medium is directly attached to the CaF$_2$ spacer, creating a better thermal contact for efficient cooling, which reduces thermally induced mode distortions. Also, the monolithic cavity design makes the MMLL compact, robust, requires no alignment, and is free from the acoustic noise peaks typically seen in solid-state lasers. The low noise performance, due to the very low round-trip loss (<1%), low net-dispersion (50..100 fs^2), and high intracavity average power make MMLLs a viable alternative for traditional OFD schemes. We recently showed that these lasers could produce X-band (8–12 GHz) microwave phase noise performance comparable to the best photonics microwave systems with significantly smaller Size, Weight, and Power (SWaP). The reported noise floor reached −178 dBc/Hz phase noise floor at offset frequencies >50 kHz from the 8 GHz carrier [4].

The phase noise floor of photonic microwave generation is usually limited by the thermal noise of the system or by the excess noise from the photodiode, which can be orders of magnitude higher than the shot-noise limit imposed by ultrashort pulse detection [14]. Characterization of microwave phase noise closer to the thermal noise is also challenging due to the collapse of the cross-spectral function, which could significantly underestimate the actual phase noise of the oscillator [15,16]. In the following, we demonstrate and characterize a record low photonic microwave phase noise from a free-running MMLL with a noise floor of −183 dBc/Hz below 1 MHz offset from the carrier in X-band. To the best of our knowledge, this is the lowest photonic microwave phase noise floor achieved in X-band carrier with a free-running photonic oscillator. We also report on a few important steps that need to be taken by all OFD systems to reach such low noise floors. A cryogenically cooled splitter was used to mitigate the cross-spectral collapse and avoid underestimating the actual phase nose.

2. Experiment and results

The experimental setup of the microwave generation and characterization setup is shown in Fig. 1. We used a free-running MMLL with a 1-GHz repetition rate. This free-running laser served as the low noise oscillator for the microwave generation setup. The microwave generation setup did not employ a high-finesse reference cavity, and detection of the carrier-envelope offset frequency of the laser was not required for this compact scheme. The laser cavity was a CaF$_2$ spacer combined with an Er:Yb:glass gain medium and a semiconductor saturable absorber mirror (SESAM). The excellent transparency and near-zero dispersion of CaF$_2$ spacer at 1550 nm grant low intrinsic noise levels for the laser. For this experiment, the output of MMLL was a sech^2-shaped pulse train centered at 1558 nm wavelength and with an average power of 35 mW. The details of this MMLL can be found in the Ref. [12].

We redirected about 2% of the laser output to an InGaAs photodiode for relative intensity noise (RIN) measurement and suppression with a bandwidth of about 30 kHz. The rest was seeding a bidirectionally pumped low noise Er-doped fiber amplifier to increase the power of the pulse train up to ~130 mW of average power. This amplified pulse train was sent through a 3-stage optical pulse inter-leaver to multiply the repetition rate by a factor 8. Each interleaving stage divided the pulse train into two beams via a polarized beam splitter and a half-wave plate. One beam was delayed by half of the interval of the incoming pulse train and recombined to subsequent double the repetition rate in each interleaver stage. The repetition rate multiplication reduced the peak power of the pulses, which in return reduced the saturation effects and the noise floor of the photodetection [17,18]. The interleaved pulse train was then coupled into a single-mode fiber for photodetection with a modified uni-traveling-carrier (MUTC) photodiode [19]. The average optical power on the photodiode was about 35 mW. The MUTC was reverse biased to the AM-PM null point using a low noise voltage source to minimize the AM-PM conversion [20,21]. The AM-PM conversion factor was measured by adding an AM tone to the optical pulse train. A 5 Ohm shunt resistor and a low noise instrumentation amplifier measured the amplitude noise of the MUTC photocurrent. A noise eater feeding into an AOM placed in front of the MUTC
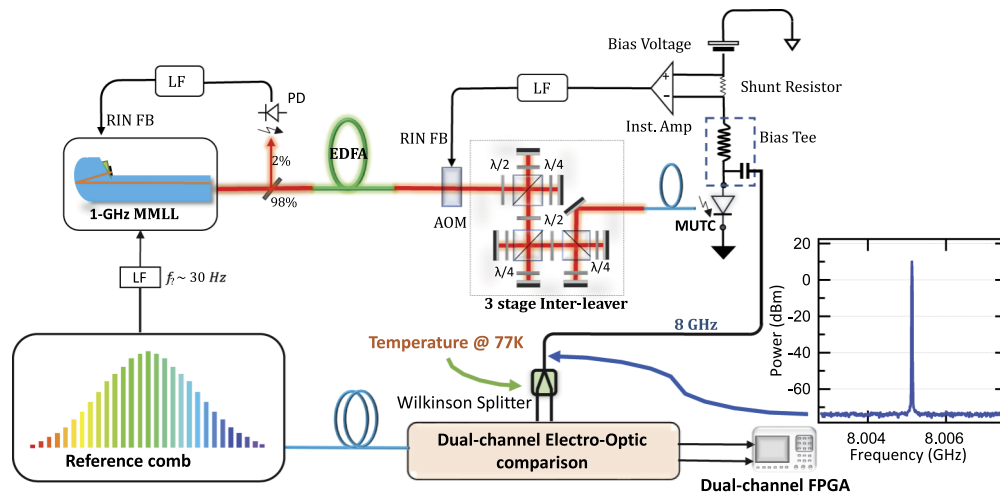
Fig. 1. Experimental setup of microwave generation and characterization. Inset at right: The 8 GHz microwave carrier power measured at the input of the power splitter. The noise floor of the inset was limited by the analyzer (Keysight N9030A PXA). The Wilkinson power splitter was cooled to 77 K with liquid Nitrogen to prevent the cross-spectrum collapse described in the text. The 8-GHz carrier power at the input of the splitter was +10 dBm. MMLL: monolithic mode-locked laser, EDFA: erbium doped fiber amplifier, RIN FB: relative intensity noise feedback, MUTC: modified uni traveling carrier photodiode, FPGA: field programmable gate array, LF: loop filter

detector was used to further suppress the optical (and the RF) AM noise and the associated phase noise in the X-band signal. The AOM was operated in zero-order mode and was driven by a weak amplitude-modulated 80 MHz carrier. For characterization, the 8-GHz microwave output from the MUTC was then divided into two coaxial cables using a Wilkinson power splitter. This allowed for the dual-channel electro-optic phase characterization described below. The 8 GHz power at the input of the splitter was +10 dBm (Fig. 1-inset).

We used a Mach-Zehnder modulator-based electro-optical cross-spectral comparison method to characterize the microwave signals [22]. In this method, the zero-crossings of the microwaves signal generated by the free-running MMLL were compared against an ultra-stable optical pulse train to characterize the phase noise of the microwave signal. The ultra-stable optical reference was a 500 MHz fully phase-stabilized free space solid-state OFC. This reference comb employed an f-2f interferometer to stabilize the comb's carrier-envelope offset frequency, and the repetition rate was stabilized by an optical phase-lock to a cavity-stabilized continuous-wave laser at 1556 nm [23,24]. As described by M. Endo *et al.* [19], the phase noise of a single channel was limited by instrumentation noise, such as flicker noise of the dual-output Mach-Zehnder modulator (DO-MZM, 2×2 PM EOspace), shot noise of baseband diodes, and electronic noise from baseband amplifiers. The time-averaged cross-spectrum between two channels yields the DUT phase noise independent from these uncorrelated noise terms. We used an FPGA-based sampling board to achieve ~30 dB of uncorrelated noise suppression within less than 5 minutes of averaging time (4 kHz RBW). We loosely locked the MMLL to the optical reference with a feedback loop with ~30 Hz BW to match the repetition rates during the measurement. A piezo-electric transducer glued to the side of the CaF$_2$ spacer of the MMLL was used for this purpose. A temperature control loop with a bandwidth ~ 0.1 Hz compensated the long-term drifts of MMLL during the measurement.

In thermal noise-limited phase noise measurements, the cross-spectrum technique potentially suffers from cross-spectral collapse, which can underestimate the actual noise of the DUT [15,16]. The thermal noise originating from the isolation resistor in the Wilkinson power splitter appears anti-correlated (phase inverted) between the two output channels of the splitter. At the point where the phase noise power spectral density of the DUT approaches the thermal noise spectral power density of the isolation resistor, these two noise terms can then cancel in the time-averaged cross-correlation function. If the phase noise of DUT is $\mu(t)$, and anti-correlated thermal noise at the splitter is $th(t)$, the noise of the two channels can be written as

$$ch_1(t) = a_1(t) + \mu(t) + th(t), \quad \text{and} \quad ch_2(t) = a_2(t) + \mu(t) - th(t) \tag{1}$$

where $a_1(t)$ and $a_2(t)$ are the uncorrelated added systematic noise terms of each channel. Then the cross power spectral density (PSD) after m averages can be written as [15]:

$$\left\langle S_{ch_1,ch_2} \right\rangle_m = \frac{1}{T} \left[\left\langle M(f) M^*(f) \right\rangle_m - \left\langle Th(f) Th^*(f) \right\rangle_m \right] = S_M(f) - S_{Th}(f) \tag{2}$$

where $M(f)$ and T$h(f)$ are Fourier transforms of $\mu(t)$, and $th(t)$. $\langle \ldots \rangle_m$ denotes the ensemble of m averages, and $*$ indicates the complex conjugate. T is the measurement time normalizing the PSD to 1 Hz. At the frequency where $S_M(f)$ and $S_{Th}(f)$ have the same magnitude, the cross-spectral density represented by Eq. (2) collapses to zero. Figure 2 shows the simulation and the experimental observations of this effect in photonic microwave characterization. Figure 2-(A) is a cartoon of the dual-channel electro-optical comparison scheme that was used here to characterize the phase noise performance of the device under test (DUT). Figure 2-(B) shows the simulation results for a DUT with a $1/f^2$ noise power spectral density and a +2 dBm carrier power at the splitter. The time-averaged cross-spectrum shows a dip at the frequency where the DUT noise reaches the splitter thermal noise floor. Figure 2-(C) shows the experimental observation of this cross-spectral collapse for an 8 GHz microwave signal generated from the interleaved pulse train of a free-running MMLL. The phase noise is underestimated at around 40 kHz offset. If the DUT has a phase noise floor close to the thermal noise of the splitter, the entire measured noise floor could fully or partially collapse, under-reporting the actual phase noise floor of the DUT [16]. Therefore, the cross-spectrum must be used with caution in thermal noise-limited phase noise measurements.

This cross-spectral collapse can be avoided by cooling the splitter and subsequently bringing the thermal noise of the splitter to a level sufficiently below the noise of the DUT [25]. For instance, if the splitter temperature is at liquid Nitrogen temperature (77 K), the thermal noise is ~6 dB lower than the noise at 300 K, and, at liquid helium temperature (4 K), it is ~18.8 dB lower. At higher offsets, the photonic microwave phase noise floor is ultimately limited by the 50 Ohm impedance of the MUTC detector. Hence cooling the splitter to 77 K will be sufficient to avoid the cross-spectral collapse. In the experiment, we simply submerged the splitter (Mini-Circuits, ZN2PD-02183-S+) in a 6-liter liquid nitrogen dewar. The size of the microwave characterization setup including the reference OFD was about 2300 liters. However, it should be noted that the microwave generation setup itself does not require cooling (cooling was only used for the characterization), and while the current size of the microwave generation setup is ~100 liters, the whole setup could indeed be very compact (liter-size), e.g. by replacing the free space interleaver with a waveguide-based interleaver [26] and with proper packaging of the laser and the supporting electronics. At this point, no effort was made to decrease the volume of the setup.

The fundamental limit of photonic microwave generation comes from the photodetection process related to the discrete nature of photons known as shot noise. For continuous illumination, the shot noise is treated as a time-independent Poissonian process, and the single side power spectral density of the shot noise is given by $S_i(f) = 2eI$, where e is the electron charge, and 'I' is the average photocurrent. However, in the regime of ultrashort pulse detection, it has been
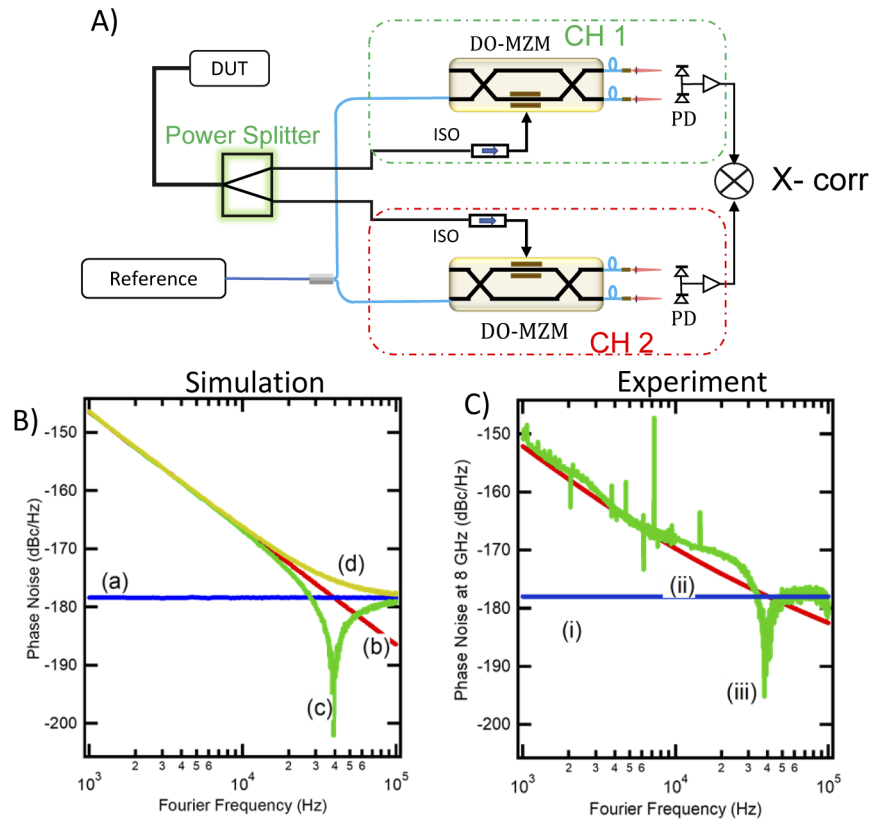
Fig. 2. The cross-spectral collapse of the dual-channel cross-correlation setup is due to the anti-correlation of thermal noise of the splitter in two channels. A) simplified dual-channel electro-optics phase noise measurement setup. DUT: Device Under Test, DO-MZM: Dual output Mach-Zehnder modulators (2×2 PM dual output, EOspace), PD: photodiodes, ISO: isolator, B) Simulation results: (a) Thermal Noise for +2 dBm carrier at the splitter, (b) DUT noise floor with $1/f^2$ noise power spectral density (c) time-averaged cross-correlation when the thermal noise appears anti-correlated between two channels. (d) without anti-correlation. C) Experimental observation in 8 GHz photonics microwave SSB phase noise characterization for a +2 dBm carrier [4]. (i) Thermal noise floor, (ii) Estimated noise of the microwave signal, (iii) Measured microwave signal with cross-spectral collapse.

shown that the noise correlations in shot noise spectrum impact the fundamental shot noise floor, enabling potentially several orders of magnitude improvement of the phase (PM) quadrature of shot noise at the cost of slight increase the amplitude (AM) noise quadrature [14,27]. The achievable shot noise improvement depends on the optical pulse width and the regular timing of the optical pulse train [28]. Figure 3-(A) shows the phase (green) and amplitude (red) quadratures of shot noise calculated from Eq. (20) in [27] for an 8 GHz sech^2 shaped pulse train for different pulse widths. Both AM and PM quadratures of the shot noise are equal to the gaussian shot noise for long pulses, but dramatic improvement of PM noise is observed for shorter pulses. However, this improvement quickly plateaus due to the collisional diffusions of the electrons in the device once the pulse width gets smaller compared to the impulse response of the photodiode (Fig. 3-(A) blue), which depends on the photodiode structure as well as the bias voltage and the photocurrent [29,30]. Recently, it has also been shown that the photodiode flicker noise shows similar pulse width dependence [31]. Figure 3-(B) shows the 3 stage interleaver used for rep

rate multiplication. Figure 3-(C) shows the phase and power deviations for non-ideal interleaver stages. For these calculations, a 200 fs sech^2 pulses train was used. The microwave phase noise floor is susceptible to interleaver errors. A 5 ps delay in one interleaver stage can increase the phase noise floor by ~20 dB with a less than 1 dB power deviation in the carrier (red curve). The green curve shows the phase noise deviation due to the second interleaver stage, if one stage already has a 5 ps error. The blue curve shows the phase noise deviation from the 3rd stage errors with 5 ps timing errors in the other two stages. To achieve more than 10 dB of PM shot noise improvement, the interleaver stage errors must be less than 5 ps.
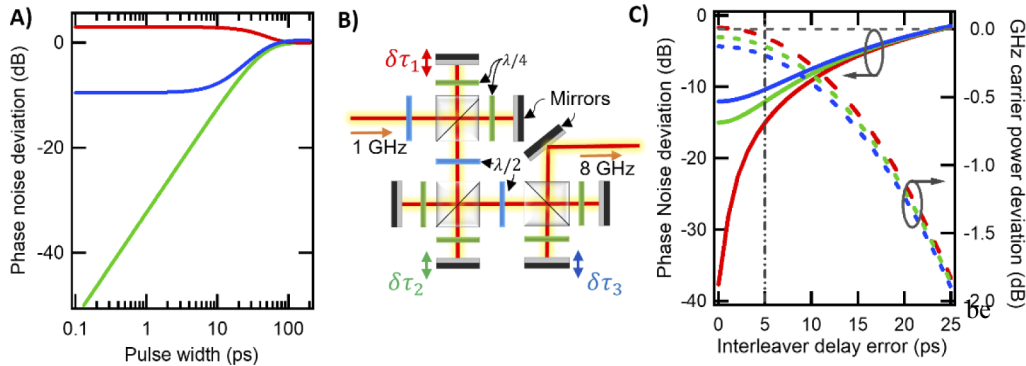

Fig. 3. Shot noise-limited phase noise deviation as a function of pulse width and inter-leaver errors. A) The shot noise limited AM (red) and PM (green) deviations for an 8 GHz, sech^2 shaped pulse train for different pulse widths. The blue curve he the phase noise deviation with an added noise floor of MUTC. B) 3-stage pulse inter-leaver for 8x pulse repetition rate multiplication. Here, $\delta\tau$ represents the inter-leaver delay error for each stage. C) shot noise-limited phase noise deviation and corresponding power deviation for the 3-stage inter-leaver at 8 GHz for a 200 fs FWHM pulse train. The red curves show the phase noise and power deviation for the delay errors at 1st stage, the green curve is for an additional delay error in the second stage (assuming a 1st-stage delay error of 5 ps.) Blue curves represent delay errors in the 3rd stage with 5 ps delay errors in both the 1st and 2nd stages.

Figure 4 summarizes the results of free-running MMLL-based 8-GHz microwave generation. The calculated free-running noise of the MMLL used for this experiment scaled to an 8 GHz carrier is shown in blue [13]. The measured flicker noise of the MUTC for the given carrier power at 8 GHz is presented in brown. Flicker noise was measured using a self-measurement, where the same MMLL laser output was used for both microwave generation and reference for the aforementioned DO-MZM-based optical sampling technique. In this configuration, the laser noise was common-mode and canceled out in the baseband. The only noise terms left were the flicker noise, the shot-noise, the 50 Ohm thermal noise, and any excess noise from non-linearities from the MUTC detector. A commercial 8 GHz YIG oscillator was used for calibrating the carrier power for this flicker noise measurement. The power splitter was cooled to 77 K during the flicker measurement to avoid the aforementioned cross-spectral collapse. The red curve shows the estimated microwave generation system performance using the MMLL noise, the MUTC flicker noise, and the photodetector thermal noise. The dashed black curve is the thermal noise of the MUTC at room temperature, which is the actual ultimate noise floor at high offsets. The violet curve shows the calculated noise floor of the reference oscillator using the in-loop signals of the Pound-Drever-Hall (PDH) lock, the repetition rate stabilization, and carrier offset stabilization. The black curve is the thermal noise of the power splitter at 77 K temperature. The orange curve shows the RIN contribution to the microwave signal. The dashed red curve shows the Poissonian shot noise for the average photocurrent. The green curve shows

the measured single-sideband phase noise of the 8 GHz photonically generated microwave carrier with free-running 1 GHz MMLL and the pulse inter-leaver. The sharp peak at 60 Hz is from the 60 Hz power line. The bump at 30 Hz is the servo bump from the repetition rate matching feedback loop with the reference comb. Note that below 30 Hz, the phase noise is in-loop with the reference comb and does not represent the actual microwave phase noise. For offsets below 100 kHz the measured microwave phase noise is about ~8 dB worse than the previously reported values in [4], which is due to the higher cavity loss and longer pulse duration of the particular MMLL used for this measurement. The bump around 900 kHz is due to the soliton-continuum interaction in the MMLL [32].

The microwave phase noise reached a state-of-the-art value of −183 dBc/Hz at an offset above 200 kHz from the 8-GHz carrier. This noise floor is above ~4 dB of the thermal noise of the MUTC. We believe this excess noise floor is due to the aforementioned photo-carrier scattering inside the photodetector and this noise floor is below ~4 dB lower than the values reported previously, which could be due to different bias voltage/photocurrents or differences in photodiode structures [28,29]. We report ~9.5 dB of PM shot noise improvement in ultrashort pulse photodetection compared to the conventional time-invariant shot noise, which is more than 4 dB better than the value shown by F. Quinlan *et al.* [14]. One drawback of the free running
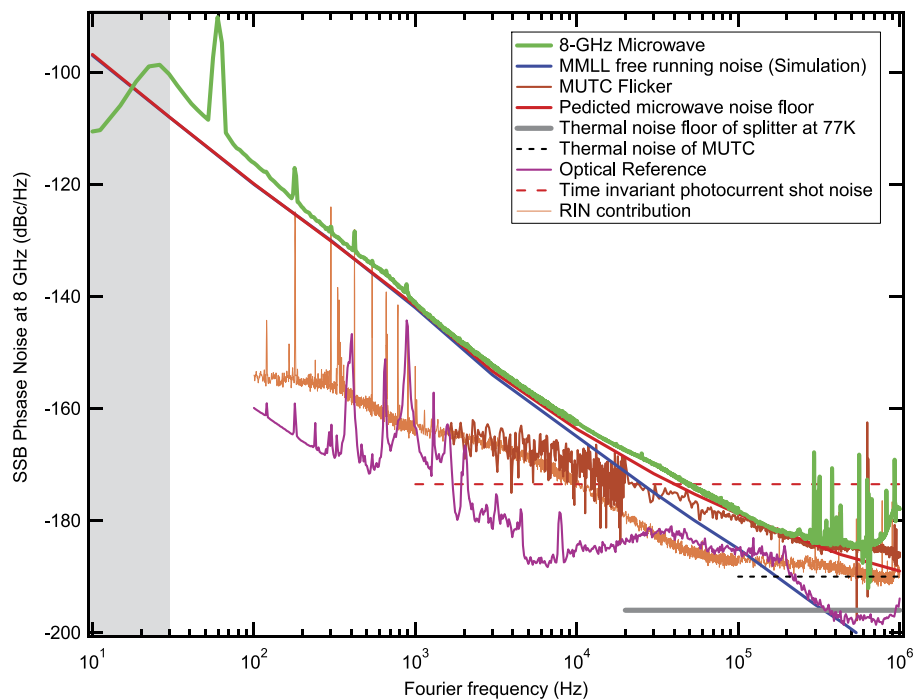
Fig. 4. Microwave generation results. The green curve shows the 8 GHz microwave single-sideband phase noise. The brown curve is the measured flicker noise of the MUTC photodiode. The blue curve shows the simulated noise of the free-running monolithic laser projected to an 8 GHz carrier. The solid red curve shows the expected phase noise of the microwave generation system. The purple curve shows the measurement limit derived from the optical reference. The red dashed curve is the long pulse shot noise floor. The grey curve is the thermal noise floor at the power splitter at 77 K. The dashed black curve is the thermal noise of MUTC. The orange curve represents the RIN contribution. The dashed red curve is the time-invariant shot noise derived from photocurrent. The shaded area represents the loop bandwidth of the repetition rate lock.

MMLL based microwave generation approach comes from the non-zero temperature coefficient of the CaF$_2$, which reduces the long-term stability of the oscillator. However, this could be improved by locking the system to an external reference.

3. Conclusion

In conclusion, we demonstrated and characterized 8 GHz photonic microwaves with SSB phase noise below −180 dBc/Hz using a free-running monolithic optical frequency comb. This is the lowest photonics-based X-band microwave phase noise floor achieved with a free-running oscillator to the best of our knowledge. We used a cryogenically cooled power splitter for an electro-optic cross-spectral characterization of the microwaves to avoid underreporting the phase noise floor. Above 100 kHz, the achievable phase noise was limited by the photocarrier scattering of the MUTC device. Improved detector designs to reduce photocarrier scattering noise could further improve photonic microwave phase noise performance [29].

Disclosures. The authors declare no competing interests.

Data availability. Data underlying the results presented in this paper are not publicly available at this time but may be obtained from the authors upon reasonable request.

References

1. X. Xie, R. Bouchand, D. Nicolodi, M. Giunta, W. Hänsel, M. Lezius, A. Joshi, S. Datta, C. Alexandre, M. Lours, P.-A. Tremblin, G. Santarelli, R. Holzwarth, and Y. Le Coq, "Photonic microwave signals with zeptosecond-level absolute timing noise," Nat. Photonics **11**(1), 44–47 (2017).
2. T. M. Fortier, M. S. Kirchner, F. Quinlan, J. Taylor, J. C. Bergquist, T. Rosenband, N. Lemke, A. Ludlow, Y. Jiang, C. W. Oates, and S. A. Diddams, "Generation of ultrastable microwaves via optical frequency division," Nat. Photonics **5**(7), 425–429 (2011).
3. T. Nakamura, J. Davila-Rodriguez, H. Leopardi, J. A. Sherman, T. M. Fortier, X. Xie, J. C. Campbell, W. F. McGrew, X. Zhang, Y. S. Hassan, D. Nicolodi, K. Beloy, A. D. Ludlow, S. A. Diddams, and F. Quinlan, "Coherent optical clock down-conversion for microwave frequencies with 10−18 instability," Science **368**(6493), 889–892 (2020).
4. M. Kalubovilage, M. Endo, and T. R. Schibli, "Ultra-low phase noise microwave generation with a free-running monolithic femtosecond laser," Opt. Express **28**(17), 25400–25409 (2020).
5. S. Koenig, D. Lopez-Diaz, J. Antes, F. Boes, R. Henneberger, A. Leuther, A. Tessmann, R. Schmogrow, D. Hillerkuss, R. Palmer, T. Zwick, C. Koos, W. Freude, O. Ambacher, J. Leuthold, and I. Kallfass, "Wireless sub-THz communication system with high data rate," Nat. Photonics **7**(12), 977–981 (2013).
6. H. Bergeron, L. C. Sinclair, W. C. Swann, C. W. Nelson, J.-D. Deschênes, E. Baumann, F. R. Giorgetta, I. Coddington, and N. R. Newbury, "Tight real-time synchronization of a microwave clock to an optical clock across a turbulent air path," Optica **3**(4), 441–447 (2016).
7. P. Ghelfi, F. Laghezza, F. Scotti, G. Serafino, A. Capria, S. Pinna, D. Onori, C. Porzi, M. Scaffardi, A. Malacarne, V. Vercesi, E. Lazzeri, F. Berizzi, and A. Bogoni, "A fully photonics-based coherent radar system," Nature **507**(7492), 341–345 (2014).
8. F. R. Giorgetta, W. C. Swann, L. C. Sinclair, E. Baumann, I. Coddington, and N. R. Newbury, "Optical two-way time and frequency transfer over free space," Nat. Photonics **7**(6), 434–438 (2013).
9. J. Kim, J. A. Cox, J. Chen, and F. X. Kärtner, "Drift-free femtosecond timing synchronization of remote optical and microwave sources," Nat. Photonics **2**(12), 733–736 (2008).
10. J. Millo, M. Abgrall, M. Lours, E. M. L. English, H. Jiang, J. Guéna, A. Clairon, M. E. Tobar, S. Bize, Y. Le Coq, and G. Santarelli, "Ultralow noise microwave generation with fiber-based optical frequency comb and application to atomic fountain clock," Appl. Phys. Lett. **94**(14), 141105 (2009).
11. L. C. Sinclair, J.-D. Deschênes, L. Sonderhouse, W. C. Swann, I. H. Khader, E. Baumann, N. R. Newbury, and I. Coddington, "Invited Article: A compact optically coherent fiber frequency comb," Rev. Sci. Instrum. **86**(8), 081301 (2015).
12. T. D. Shoji, W. Xie, K. L. Silverman, A. Feldman, T. Harvey, R. P. Mirin, and T. R. Schibli, "Ultra-low-noise monolithic mode-locked solid-state laser," Optica **3**(9), 995–998 (2016).
13. M. Endo, T. D. Shoji, and T. R. Schibli, "Ultralow Noise Optical Frequency Combs," IEEE J. Sel. Top. Quantum Electron. **24**(5), 1–13 (2018).

14. F. Quinlan, T. M. Fortier, H. Jiang, A. Hati, C. Nelson, Y. Fu, J. C. Campbell, and S. A. Diddams, "Exploiting shot noise correlations in the photodetection of ultrashort optical pulse trains," Nat. Photonics **7**(4), 290–293 (2013).

15. C. W. Nelson, A. Hati, and D. A. Howe, "A collapse of the cross-spectral function in phase noise metrology," Rev. Sci. Instrum. **85**(2), 024705 (2014).

16. C. W. Nelson, A. Hati, and D. A. Howe, "Cross-spectral collapse from anti-correlated thermal noise in power splitters," in *2016 European Frequency and Time Forum (EFTF)* (IEEE, 2016), pp. 1–4.

17. S. A. Diddams, M. Kirchner, T. Fortier, D. Braje, A. M. Weiner, and L. Hollberg, "Improved signal-to-noise ratio of 10 GHz microwave signals generated with a mode-filtered femtosecond laser frequency comb," Opt. Express **17**(5), 3331–3340 (2009).

18. H. Jiang, J. Taylor, F. Quinlan, T. Fortier, and S. A. Diddams, "Noise Floor Reduction of an Er:Fiber Laser-Based Photonic Microwave Generator," IEEE Photonics J. **3**(6), 1004–1012 (2011).

19. A. Beling, X. Xie, and J. C. Campbell, "High-power, high-linearity photodiodes," Optica **3**(3), 328–338 (2016).

20. W. Zhang, T. Li, M. Lours, S. Seidelin, G. Santarelli, and Y. Le Coq, "Amplitude to phase conversion of InGaAs pin photo-diodes for femtosecond lasers microwave signal generation," Appl. Phys. B **106**(2), 301–308 (2012).

21. Z. Li, H. Pan, H. Chen, A. Beling, and J. C. Campbell, "High-Saturation-Current Modified Uni-Traveling-Carrier Photodiode With Cliff Layer," IEEE J. Quantum Electron. **46**(5), 626–632 (2010).

22. M. Endo, T. D. Shoji, and T. R. Schibli, "High-sensitivity optical to microwave comparison with dual-output Mach-Zehnder modulators," Sci Rep **8**(1), 4388 (2018).

23. R. W. P. Drever, J. L. Hall, F. V. Kowalski, J. Hough, G. M. Ford, A. J. Munley, and H. Ward, "Laser phase and frequency stabilization using an optical resonator," Appl. Phys. B **31**(2), 97–105 (1983).

24. M. Endo and T. R. Schibli, "Residual phase noise suppression for Pound-Drever-Hall cavity stabilization with an electro-optic modulator," OSA Continuum **1**(1), 116–123 (2018).

25. A. Hati, C. W. Nelson, D. P. Pappas, and D. A. Howe, "Phase noise measurements with a cryogenic power-splitter to minimize the cross-spectral collapse effect," Rev. Sci. Instrum. **88**(11), 114707 (2017).

26. M. Y. Sander, S. Frolov, J. Shmulovich, E. P. Ippen, and F. X. Kärtner, "10 GHz femtosecond pulse interleaver in planar waveguide technology," Opt. Express **20**(4), 4102–4113 (2012).

27. F. Quinlan, T. M. Fortier, H. Jiang, and S. A. Diddams, "Analysis of shot noise in the detection of ultrashort optical pulse trains," J. Opt. Soc. Am. B **30**(6), 1775–1785 (2013).

28. F. Quinlan, F. N. Baynes, T. M. Fortier, Q. Zhou, A. Cross, J. C. Campbell, and S. A. Diddams, "Optical amplification and pulse interleaving for low-noise photonic microwave generation," Opt. Lett. **39**(6), 1581–1584 (2014).

29. S. E. J. Mahabadi, S. Wang, T. F. Carruthers, C. R. Menyuk, F. J. Quinlan, M. N. Hutchinson, J. D. McKinney, and K. J. Williams, "Calculation of the impulse response and phase noise of a high-current photodetector using the drift-diffusion equations," Opt. Express **27**(3), 3717–3730 (2019).

30. W. Sun, F. Quinlan, T. M. Fortier, J.-D. Deschenes, Y. Fu, S. A. Diddams, and J. C. Campbell, "Broadband Noise Limit in the Photodetection of Ultralow Jitter Optical Pulses," Phys. Rev. Lett. **113**(20), 203901 (2014).

31. D. Lee, T. Nakamura, J. Zang, J. C. Campbell, S. A. Diddams, and F. Quinlan, "Reduction of Flicker Phase Noise in High-Speed Photodetectors Under Ultrashort Pulse Illumination," IEEE Photonics J. **13**(3), 1–12 (2021).

32. C.-C. Lee and T. R. Schibli, "Intrinsic Power Oscillations Generated by the Backaction of Continuum on Solitons and its Implications on the Transfer Functions of a Mode-Locked Laser," Phys. Rev. Lett. **112**(22), 223903 (2014).